Atmos. Meas. Tech. Discuss., 5, 2395–2413, 2012
www.atmos-meas-tech-discuss.net/5/2395/2012/
doi:10.5194/amtd-5-2395-2012

Atmospheric Measurement Techniques Discussions

Dimethylamine and ammonia measurements with ion chromatography during the CLOUD4 campaign

A. P. Praplan, F. Bianchi, J. Dommen, and U. Baltensperger

Laboratory of Atmospheric Chemistry, Paul Scherrer Institute, Villigen PSI, Switzerland

Received: 3 February 2012 – Accepted: 2 March 2012 – Published: 23 March 2012

Correspondence to: J. Dommen (josef.dommen@psi.ch)

Published by Copernicus Publications on behalf of the European Geosciences Union.

Abstract

The CLOUD project investigates the influence of galactic cosmic rays on the nucleation of new particles in an environmental chamber at CERN. Ion chromatography was utilised together with a sampling device developed for CLOUD in order to measure ammonia (NH_3) and dimethylamine (DMA) at low pptv levels. Sampling was performed by dissolving the gaseous NH_3 and DMA, which were protonated and retained on trace cation concentrator columns as ammonium and dimethylaminium with an efficiency well above 95 %. The sampling time varied between 70 and 210 min. A longer sampling time allowed a decrease of the detection limit for each species down to the sub-pptv level.

NH_3 mixing ratios reported were initially high du to an unintentional injection of NH_3. They then recovered to background levels around 10 pptv, with no further injection of NH_3. DMA was injected intentionally to reach atmospherically relevant levels away from sources (up to 60 pptv) in order to study its effect on nucleation with sulphuric acid and water at 278 K.

1 Introduction

The CLOUD project investigates the influence of galactic cosmic rays (GCR) on the climate through their effect on cloud properties (Kirkby, 2007). A key process of these studies is the nucleation of new particles in the atmosphere from gaseous precursors and their growth to detectable sizes (>3 nm) (Kulmala et al., 2004; Hirsikko et al., 2011). These particles can eventually grow to cloud condensation nuclei (CCN) and influence indirectly the Earth's climate by modifying cloud properties. Recently published CLOUD3 data (Kirkby et al., 2011) on the ternary sulphuric acid (H_2SO_4)/water (H_2O)/ammonia (NH_3) nucleation system (Coffman and Hegg, 1995; Korhonen et al., 1999; Kulmala et al., 2000), demonstrated that NH_3 (at a 100 pptv-level or less) increases nucleation rates by a factor higher than 100 to 1000 over the

AMTD
5, 2395–2413, 2012

binary (H_2SO_4/H_2O) system. However, NH_3 was still not sufficient to explain the nucleation rates observed under typical tropospheric conditions (10^6–10^7 cm^{-3} H_2SO_4).

Because amines possess structural similarities with NH_3 where one, two or all three hydrogen atoms are replaced by organic moieties (RNH_2, R_2NH or R_3N), their effect on secondary organic aerosol formation is increasingly subject of investigation. Murphy et al. (2007) showed that amines can form secondary organic aerosol (SOA), by acting as bases and neutralising acids present in the gas phase similar to NH_3, but also by participating in gas phase chemistry initiated by hydroxyl radicals ($OH^{\cdot}$) or ozone (O_3) to form low volatility products (see also Tuazon et al., 1994). Furthermore, a recent computational study suggests that amines are even more strongly bound to H_2SO_4 molecules than NH_3 (Kurtén et al., 2008) and can therefore enhance even more neutral and ion-induced H_2SO_4/H_2O nucleation in the atmosphere. Bzdek et al. (2010) found experimental evidence for this effect: even at pptv-levels, complete displacement of NH_3 by dimethylamine (DMA) occurs within seconds or minutes, changing the composition of sub-3 nm diameter bisulphate clusters. Not only substitution, but also addition to those clusters can occur, influencing their growth rates (Bzdek et al., 2011). Mäkelä et al. (2001) found that DMA was present at higher mixing ratios during nucleation events in boreal forests compared to non-event periods, making it a potential nucleating species or a species increasing growth rates of freshly formed particles, so that they can be detected faster at 3 nm. Yu et al. (2012) also reported enhancement effects on the nucleation rate by several amines.

CLOUD4 (June–July 2011) investigated the role of DMA in the formation and growth of new particles. Ion chromatography (IC) is a method often used to analyse amines and inorganic cations like ammonium (NH_4^+) from atmospheric samples with various sampling methods (Mäkelä et al., 2001; Murphy et al., 2007; VandenBoer et al., 2011) and was employed for this work. The particular sampling device and the IC method used for quantitative analysis are described hereafter along with the results of the measurements performed for CLOUD4.

AMTD
5, 2395–2413, 2012

2 Experimental

2.1 CLOUD chamber

The CLOUD chamber is a 26.1 m^3 electropolished stainless steel cylinder. A more detailed description can be found in Voigtländer et al. (2012) and Kirkby et al. (2011). The fibre-optic UV system for H_2SO_4 production with negligible thermal effect is described in Kupc et al. (2011). Although the chamber temperature can be varied from 183 to 313 K, it was kept constant at 278 K (±0.05 K) with a relative humidity of 38 % (±0.1 %) during CLOUD4.

2.2 Sampling of NH_3 and DMA

The same sampling probe as the one described in Bianchi et al. (2012) was used (Fig. 1). It was specially designed to minimise the loss of NH_3 and amines on surfaces. Briefly, it consists of a 2-mm diameter stainless steel tubing of 140 cm length with a small orifice to the CLOUD chamber. Ultra pure water (18.2 MΩ cm) was introduced by a peristaltic pump in the stainless steel tubing (0.25–0.80 ml min^{-1}). A cation trap column (CTC-2, Dionex) was additionally used to remove the possibly interfering cations from this water prior to sampling. As the water reached the orifice to the CLOUD chamber, it was mixed with air (0.8–2.1 l min^{-1}) in a 10-loop coil to allow for dissolution of the gaseous species into the water. With this setup only a section of 5 mm tubing remained unflushed by water, so that sampling losses became negligible.

A debubbler separates the air and the water, which is pumped from the bottom of the debubbler by a peristaltic pump. This water was passed through a trace cation concentrator column (TCC-2 or TCC-LP1, Dionex), where cations were retained. After 70 to 210 min of sampling, the 10-port valve described in Fig. 2 rotated to allow the elution of the cations to the analytical column while the sampling water was concentrated on a second cation concentrator column to ensure continuous measurements. This automatisation was necessary as the CLOUD chamber cannot be accessed at all times

AMTD
5, 2395–2413, 2012

(e.g. when it is irradiated by the pion beam) and it reduced the required maintenance to a minimum. No derivatisation was needed and the samples could be directly eluted to the analytical column automatically at the end of the sampling period.

To test the sampling efficiency for NH_3 and amines, a second scrubbing system was installed in series at the end of the campaign as shown in the lower part of Fig. 1. It consisted of a Teflon® tubing of 1 mm diameter and 140 cm length. The air flow used for this setup was 1 l min^{-1} and both liquid flows were 0.5 ml min^{-1}. The sampling was alternated from one debubbler to the other using the valve system described previously.

2.3 Ion chromatography (IC)

A Dionex DX600 system was used for the analysis of the collected cations with Ionpac® CG10 and Ionpac® CS10 (Dionex) guard and analytical columns, respectively. The method used was similar to the one described in Chang et al. (2003): Samples were eluted with 40 mM methanesulfonic acid (MSA) at 1 ml min^{-1} (isocratic). Retention times varied between 8.8 and 10.5 min for NH_3 and between 17.8 and 21.1 min for DMA. The peaks obtained from the conductivity detector were integrated manually. Calibration was performed by direct injection of aqueous standards (no preconcentration) of different concentration levels, corresponding to injected amounts ranging from 0 to 30 ng for NH_3 and 0 to 150 ng for DMA (Fig. 3).

The method detection limit (MDL) depends primarily on the noise of the chromatograms, but is influenced by the sample volume (based on sampling air flow and sampling time). Depending on instrumental conditions and sampling time, the MDL ranged from 0.2 to 3.7 pptv for NH_3 and from 0.2 to 1.0 pptv for DMA (signal/noise = 3).

AMTD
5, 2395–2413, 2012

3 Results and discussion

3.1 Sampling efficiency

The use of pure water without addition of an acidic compound is assumed to be sufficient for measurements of low mixing ratios of NH_3 and DMA (<100 pptv). From a theoretical point of view, the sampling efficiency relies on the effective Henry's Law constant, H^*, which depends on the degree of protonation of the species in solution and thus on pH ($-\log[H^+]$). Equation (1) defines H^*, taking into account the pH of the solution and the dissociation constant, K_a, of the analytes. The negative logarithm of the dissociation constant (pK_a) of NH_4^+ is 9.90 at 278 K (Bates and Pinching, 1950) and the one of dimethylaminium ($DMAH^+$) is 10.64 at 293 K (Hall, 1957).

$$H^* = H(1 + 10^{-\mathrm{pH}+pK_a}) = \frac{[B] + [BH^+]}{p_B}, \quad (1)$$

where p_B is the partial pressure of base (B) in the gas phase. From the review of Sander (1999), Henry's law constants at 278 K are estimated to be in the range of 14.3–173 M atm^{-1} for NH_3 and 81.3–150 M atm^{-1} for DMA. At this temperature, Hawkes (1995) reports a negative logarithm of the self-ionisation constant of water ($pK_w = -\log([H^+][OH^-])$ of 14.7, corresponding to a pH of 7.3 for pure water (H_2SO_4 can be neglected). This value can increase up to 7.5 by dissolving low gas phase concentrations of DMA and NH_3 (<100 pptv each), assuming complete dissolution. Moreover, the degree of protonation of both species in solution is higher than 99 % (Eq. 2) at pH 7.5:

$$\frac{[B]}{[BH^+]} = 10^{\mathrm{pH}-pK_a} \quad (2)$$

Therefore [B] can be neglected in Eq. (1) and because p_B is equal to the difference between the total amount of B in the system (here 100 pptv) and $[BH^+]$, p_B and $[BH^+]$ can be derived from Eq. (1). Considering pure solutions of each species, the amount

AMTD
5, 2395–2413, 2012

remaining in the gas phase (p_B) is between 0.35 and 4.1 % for NH_3 and between 0.06 and 0.12 % for DMA. Under these conditions the sampling efficiency is therefore expected to be higher than 95 % overall. These calculations assumed a liquid to air flow ratio of 0.25×10^{-3} in the sampling line. This ratio influences the sampling efficiency as depicted in Fig. 4. The value of the ratio throughout the experiment is presented on the left, while the values obtained by varying the liquid to air flow ratio for a constant DMA mixing ratio in the chamber (around 60 pptv) are depicted on the right.

If the ratio drops below 0.25×10^{-3}, the sampling efficiency decreases, indicating that the stripping efficiency is governed by the residence time and not the gas-liquid equilibrium. Because some data were recorded with a ratio lower than 0.25×10^{-3}, they were corrected accordingly.

Because NH_3 was not injected at a constant mixing ratio into the chamber, the same test could not be done. Furthermore, at the end of the campaign, a second sampling system was set in series with the first one as shown in Fig. 1. No DMA could be detected in the water sampled from the second system. Because the measured concentration was close to 60 pptv and the detection limit 0.6 pptv, the sampling efficiency is at least 99 %. Unfortunately, the second system was contaminated with NH_3, so that no reliable conclusion can be drawn for this species.

3.2 IC method

The use of the CS10 analytical column from Dionex allowed the separation of NH_3 and DMA without any interference of the peaks on each other, even when both species have very different concentration levels, which can often be problematic (VandenBoer et al., 2011). This was possible because of the cleanliness of the CLOUD chamber and the absence of interfering peaks. Only sodium and potassium peaks also appeared in the chromatograms but well resolved from the peaks of interest.

AMTD
5, 2395–2413, 2012

3.3 NH_3 and DMA mixing ratios

Figures 5 and 6 summarise the measured mixing ratios for NH_3 and DMA determined with IC. The instrument was not used at the very beginning of the campaign and no reliable data could be acquired between 6 and 11 July, due to an elevated conductivity background, which increased the MDL.

Blank values were obtained by directly sampling water instead of flushing it through the sampling line. No peak for DMA could be observed from these measurements during the whole campaign, so that no correction was applied to the obtained mixing ratio. On the other hand, NH_3 showed peaks in the blank samples during the second phase of the campaign (after 11 July, when the sampling time was extended) and the measured mixing ratios were corrected proportionally to the water amount concentrated on the column (which depends on water flow and sampling time) for this period.

Figure 5 shows the uncorrected mixing ratios of NH_3, as well as the ones corrected for background levels from the sampling water. To take into account the previous discussion about sampling efficiency, the data before 1 July (marked with green color) were corrected by a factor 2, because the liquid to air flow ratio was around 0.15×10^{-3}. In the night from 2 to 3 July, this ratio dropped again below 0.25×10^{-3}, but no NH_3 data could be acquired due to an interference in the chromatograms.

The NH_3 mixing ratio ranged mostly below 20 pptv, which corresponds to mixing ratios found at remote locations (Krupa, 2003). Some values at the beginning of the measurements show higher values. This is due to an unintentional injection of NH_3. After several days of experiment, where the air sampled from the CLOUD chamber was continuously replaced by NH_3-free air, the NH_3 mixing ratios decreased to values around 10 pptv. This corresponded to the background level of NH_3 at the present conditions.

The top panel of Fig. 6 shows the mass flow controller settings for continuous DMA injection into the CLOUD chamber. It was expected that the DMA levels were proportional to these settings. Indeed, the mixing ratios shown on the bottom panel of Fig. 6

AMTD
5, 2395–2413, 2012

followed this trend. However, after switching back from higher settings to lower ones, the measured mixing ratio did not drop to previous levels but showed a background of a few pptv, slowly decreasing. Data were multiplied by a factor 2 when the liquid to air flow ratio was around 0.15×10^{-3} (before 1 July) and by a factor 1.5 when the ratio was around 0.2×10^{-3} (in the night from 2 to 3 July), as previously discussed. The values reported for both species were in some cases very close to the MDL, in particular in the period from 21 to 24 July.

With the sampling system used, no separation of the gas and aerosol phase occurred. For total aerosol mass loadings higher than $1\,\mu g\,m^{-3}$, corrections may need to be considered, to take into account the ammonium and dimethylaminium from the particle phase.

DMA mixing ratios correspond to atmospherically relevant levels away from the sources (Ge et al., 2011). On the other hand, NH_3 atmospheric levels range from a few hundreds of pptv to several ppbv (Li et al., 2006; Benson et al., 2010). Lower values could usually not be reported because of detection limitations.

4 Conclusions and outlook

The analysis of trace gases at pptv-level (ca. $10^7\,cm^{-3}$) is crucial for the understanding of nucleation because such levels of certain contaminants (e.g. NH_3, organics) can be sufficient to enhance nucleation rates by several orders of magnitude. The method presented here, based on IC and making use of an efficient sampling line, could provide data down to sub-pptv levels with 70 to 210 min time resolution.

Studies at low temperature also need to be performed. However, for CLOUD campaigns below 273 K, the sampling line needs to be adapted so that water does not freeze in the sampling line.

Grönberg et al. (1992) reported 0.5 and 1.8 pptv of DMA in urban and rural environments in Sweden. Chang et al. (2003) measured a broader range and slightly higher mixing ratios of DMA (1.9–34 pptv) at a suburban site in Seoul, Korea. Closer to

AMTD
5, 2395–2413, 2012

agricultural sources, Schade and Crutzen (1995) found outdoor mixing ratios of DMA of 21 pptv in the afternoon and 76 pptv just before sunrise. The levels of DMA injected into the CLOUD chamber represented well that range. Moreover, in all those studies, methylamine and trimethylamine were also present at similar levels (low pptv levels to a few hundreds of pptv). Akyüz (2007) found DMA levels of approximately 10 pptv without large variation between summer and winter in six sampling sites in the Zonguldak province, Turkey, as well as strongly varying concentrations of various other amines.

Usually, NH_3 is also present at several orders of magnitude higher levels (ppbv) than the individual amines. VandenBoer et al. (2011) reported amines to NH_3 ratios in Toronto between 1.6–20 $\times$ 10^{-3}, while this ratio ranged from 4.6 $\times$ 10^{-3} to 11 during the CLOUD4 campaign. The influence of such a level of DMA on nucleation and growth rates in the presence of low NH3 mixing ratio will be the subject of other publications.

Acknowledgements. This work was supported by the Swiss National Science Foundation (project nos. 200020_135307 and 206620_130527) and by the EC Seventh Framework project CLOUD-ITN (MC-Initial Training Network No. 215072).

References

Akyüz, M.: Simultaneous determination of aliphatic and aromatic amines in indoor and outdoor air samples by gas chromatography-mass spectrometry, Talanta, 71, 486–492, doi:10.1016/j.talanta.2006.10.028, 2007. 2404

Bates, R. G. and Pinching, G. D.: Dissociation constant of aqueous ammonia at 0 to 50° from e.m.f. studies of the ammonium salt of a weak acid, J. Am. Chem. Soc., 72, 1393–1396, doi:10.1021/ja01159a087, 1950.

Benson, D. R., Markovich, A., Al-Refai, M., and Lee, S.-H.: A chemical ionization mass spectrometer for ambient measurements of ammonia, Atmos. Meas. Tech., 3, 1075–1087, doi:10.5194/amt-3-1075-2010, 2010. 2403

Bianchi, F., Dommen, J., Mathot, S., and Baltensperger, U.: On-line determination of ammonia at low pptv mixing ratios in the CLOUD chamber, Atmos. Meas. Tech. Discuss., 5, 2111–2130, doi:10.5194/amtd-5-2111-2012, 2012. 2398

AMTD
5, 2395–2413, 2012

Bzdek, B. R., Ridge, D. P., and Johnston, M. V.: Size-dependent reactions of ammonium bisulfate clusters with dimethylamine, J. Phys. Chem. A, 114, 11638–11644, doi:10.1021/jp106363m, 2010. 2397

Bzdek, B. R., Ridge, D. P., and Johnston, M. V.: Amine reactivity with charged sulfuric acid clusters, Atmos. Chem. Phys., 11, 8735–8743, doi:10.5194/acp-11-8735-2011, 2011. 2397

Chang, I.-H., Lee, C.-G., and Lee, D. S.: Development of an automated method for simultaneous determination of low molecular weight aliphatic amines and ammonia in ambient air by diffusion scrubber coupled to ion chromatography, Anal. Chem., 75, 6141–6146, doi:10.1021/ac0347314, 2003. 2399, 2403

Coffman, D. J. and Hegg, D. A.: A preliminary study of the effect of ammonia on particle nucleation in the marine boundary layer, J. Geophys. Res., 100, 7147–7160, doi:10.1029/94JD03253, 1995. 2396

Ge, X., Wexler, A. S., and Clegg, S. L.: Atmospheric amines – Part I, A review, Atmos. Environ., 45, 524–546, doi:10.1016/j.atmosenv.2010.10.012, 2011. 2403

Grönberg, L., Lövkvist, P., and Jönsson, J.: Determination of aliphatic amines in air by membrane enrichment directly coupled to a gas chromatograph, Chromatographia, 33, 77–82, doi:10.1007/BF02276856, 1992. 2403

Hall, H. K.: Correlation of the base strengths of amines, J. Am. Chem. Soc., 79, 5441–5444, doi:10.1021/ja01577a030, 1957.

Hawkes, S. J.: pK_w is almost never 14.0: Contribution from the task force on the General Chemistry Curriculum, J. Chem. Educ., 72, p. 799, 1995.

Hirsikko, A., Nieminen, T., Gagné, S., Lehtipalo, K., Manninen, H. E., Ehn, M., Hõrrak, U., Kerminen, V.-M., Laakso, L., McMurry, P. H., Mirme, A., Mirme, S., Petäjä, T., Tammet, H., Vakkari, V., Vana, M., and Kulmala, M.: Atmospheric ions and nucleation: a review of observations, Atmos. Chem. Phys., 11, 767–798, doi:10.5194/acp-11-767-2011, 2011. 2396

Kirkby, J.: Cosmic rays and climate, Surv. Geophys., 28, 333–375, doi:10.1007/s10712-008-9030-6, 2007. 2396

Kirkby, J., Curtius, J., Almeida, J., Dunne, E., Duplissy, J., Ehrhart, S., Franchin, A., Gagné, S., Ickes, L., Kürten, A., Kupc, A., Metzger, A., Riccobono, F., Rondo, L., Schobesberger, S., Tsagkogeorgas, G., Wimmer, D., Amorim, A., Bianchi, F., Breitenlechner, M., David, A., Dommen, J., Downard, A., Ehn, M., Flagan, R. C., Haider, S., Hansel, A., Hauser, D., Jud, W., Junninen, H., Kreissl, F., Kvashin, A., Laaksonen, A., Lehtipalo, K., Lima, J., Lovejoy, E. R., Makhmutov, V., Mathot, S., Mikkilä, J., Minginette, P., Mogo, S., Nieminen, T., Onnela, A.,

AMTD
5, 2395–2413, 2012

Pereira, P., Petäjä, T., Schnitzhofer, R., Seinfeld, J. H., Sipilä, M., Stozhkov, Y., Stratmann, F., Tomé, A., Vanhanen, J., Viisanen, Y., Vrtala, A., Wagner, P. E., Walther, H., Weingartner, E., Wex, H., Winkler, P. M., Carslaw, K. S., Worsnop, D. R., Baltensperger, U., and Kulmala, M.: Role of sulphuric acid, ammonia and galactic cosmic rays in atmospheric aerosol nucleation, Nature, 476, 429–433, doi:10.1038/nature10343, 2011. 2396, 2398

Korhonen, P., Kulmala, M., Laaksonen, A., Viisanen, Y., McGraw, R., and Seinfeld, J. H.: Ternary nucleation of H_2SO_4, NH_3, and H_2O in the atmosphere, J. Geophys. Res., 104, 26349–26353, doi:10.1029/1999JD900784, 1999. 2396

Krupa, S. V.: Effects of atmospheric ammonia (NH_3) on terrestrial vegetation: a review, Environ. Pollut., 124, 179–221, doi:10.1016/S0269-7491(02)00434-7, 2003. 2402

Kulmala, M., Pirjola, L., and Mäkelä, J. M.: Stable sulphate clusters as a source of new atmospheric particles, Nature, 404, 66–69, doi:10.1038/35003550, 2000. 2396

Kulmala, M., Vehkamäki, H., Petäjä, T., Dal Maso, M., Lauri, A., Kerminen, V.-M., Birmili, W., and McMurry, P. H.: Formation and growth rates of ultrafine atmospheric particles: a review of observations, J. Aerosol Sci., 35, 143–176, doi:10.1016/j.jaerosci.2003.10.003, 2004. 2396

Kupc, A., Amorim, A., Curtius, J., Danielczok, A., Duplissy, J., Ehrhart, S., Walther, H., Ickes, L., Kirkby, J., Kürten, A., Lima, J. M., Mathot, S., Minginette, P., Onnela, A., Rondo, L., and Wagner, P. E.: A fibre-optic UV system for H_2SO_4 production in aerosol chambers causing minimal thermal effects, J. Aerosol Sci., 42, 532–543, doi:10.1016/j.jaerosci.2011.05.001, 2011. 2398

Kurtén, T., Loukonen, V., Vehkamäki, H., and Kulmala, M.: Amines are likely to enhance neutral and ion-induced sulfuric acid-water nucleation in the atmosphere more effectively than ammonia, Atmos. Chem. Phys., 8, 4095–4103, doi:10.5194/acp-8-4095-2008, 2008. 2397

Li, Y., Schwab, J. J., and Demerjian, K. L.: Measurements of ambient ammonia using a tunable diode laser absorption spectrometer: Characteristics of ambient ammonia emissions in an urban area of New York City, J. Geophys. Res., 111, D10S02, doi:10.1029/2005JD006275, 2006. 2403

Mäkelä, J. M., Yli-koivisto, S., Hiltunen, V., Seidl, W., Swietlicki, E., Teinilä, K., Sillanpää, M., Koponen, I. K., Paatero, J., Rosman, K., and Hämeri, K.: Chemical composition of aerosol during particle formation events in boreal forest, Tellus B, 53, 380–393, doi:10.1034/j.1600-0889.2001.530405.x, 2001. 2397

Murphy, S. M., Sorooshian, A., Kroll, J. H., Ng, N. L., Chhabra, P., Tong, C., Surratt, J. D., Knipping, E., Flagan, R. C., and Seinfeld, J. H.: Secondary aerosol formation from atmospheric

AMTD
5, 2395–2413, 2012

reactions of aliphatic amines, Atmos. Chem. Phys., 7, 2313–2337, doi:10.5194/acp-7-2313-2007, 2007. 2397

Sander, R.: Compilation of Henry's law constants for inorganic and organic species of potential importance in environmental chemistry (Version 3), available at: http://www.henrys-law.org, 1999.

Schade, G. W. and Crutzen, P. J.: Emission of aliphatic amines from animal husbandry and their reactions: Potential source of N_2O and HCN, J. Atmos. Chem., 22, 319–346, doi:10.1007/BF00696641, 1995. 2404

Tuazon, E. C., Atkinson, R., Aschmann, S. M., and Arey, J.: Kinetics and products of the gas-phase reactions of O_3 with amines and related compounds, Res. Chem. Intermed., 20, 303–320, doi:10.1163/156856794X00351, 1994. 2397

VandenBoer, T. C., Petroff, A., Markovic, M. Z., and Murphy, J. G.: Size distribution of alkyl amines in continental particulate matter and their online detection in the gas and particle phase, Atmos. Chem. Phys., 11, 4319–4332, doi:10.5194/acp-11-4319-2011, 2011. 2397, 2401

Voigtländer, J., Duplissy, J., Rondo, L., Kürten, A., and Stratmann, F.: Numerical simulations of mixing conditions and aerosol dynamics in the CERN CLOUD chamber, Atmos. Chem. Phys., 12, 2205–2214, doi:10.5194/acp-12-2205-2012, 2012. 2398

Yu, H., McGraw, R., and Lee, S.-H.: Effects of amines on formation of sub-3 nm particles and their subsequent growth, Geophys. Res. Lett., 39, L02807, doi:10.1029/2011GL050099, 2012. 2397

AMTD
5, 2395–2413, 2012

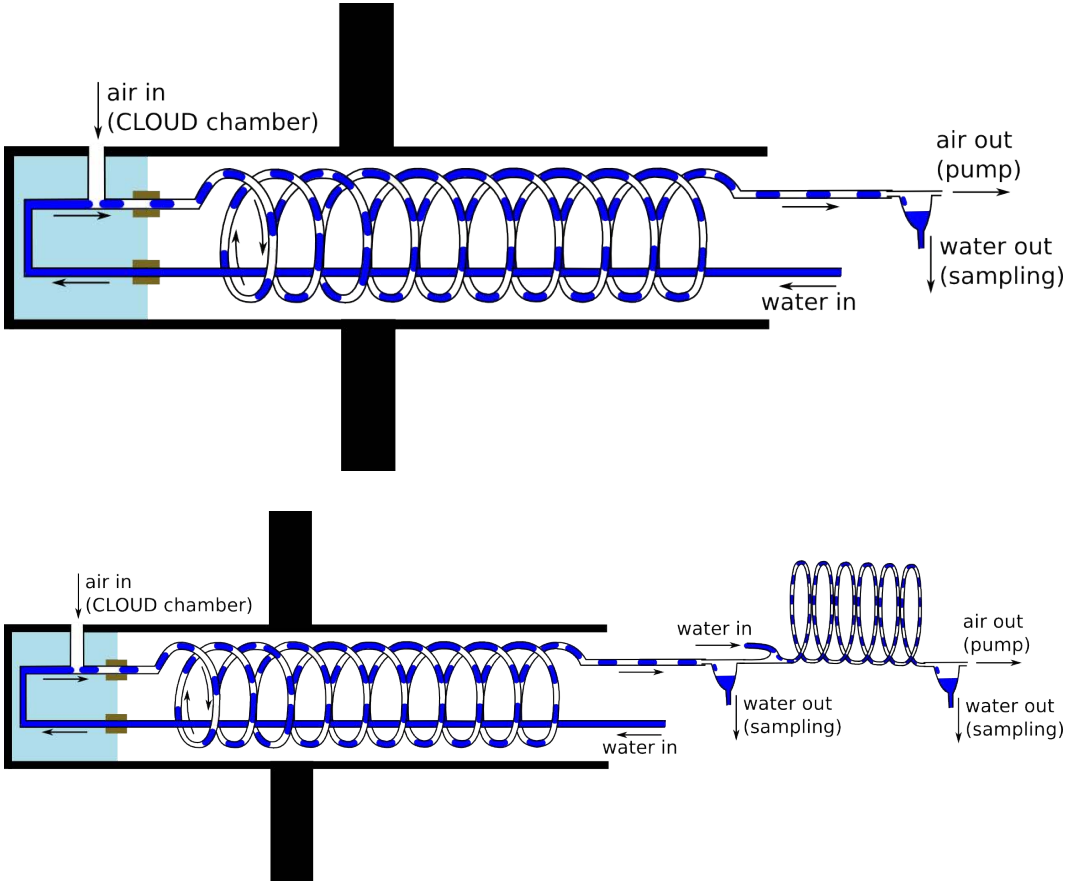

Fig. 1. Unscaled schematic of the sampling system used for CLOUD4 (top panel) and the modified sampling system with two debubblers (bottom panel) for sampling efficiency tests.

AMTD
5, 2395–2413, 2012

DMA and NH_3 measurements with IC during CLOUD4

A. P. Praplan et al.

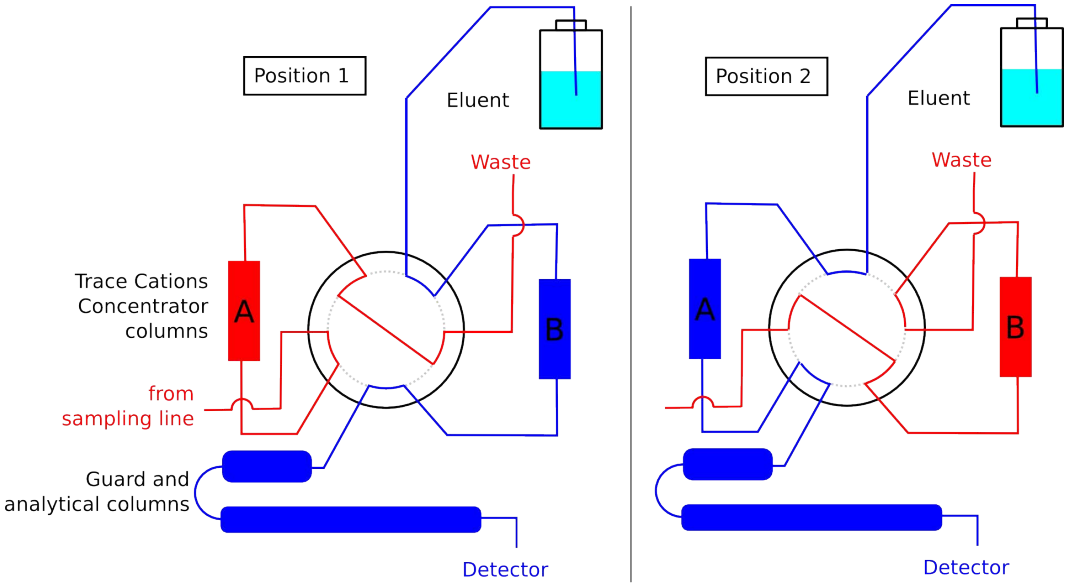

Fig. 2. Schematic of the concentrating system with two columns and a 10-port valve to ensure continuous measurements. While one column concentrates the analytes coming from the chamber sampling line (red line), the other column can be eluted and the sample analysed by ion chromatography (blue line).

AMTD
5, 2395–2413, 2012

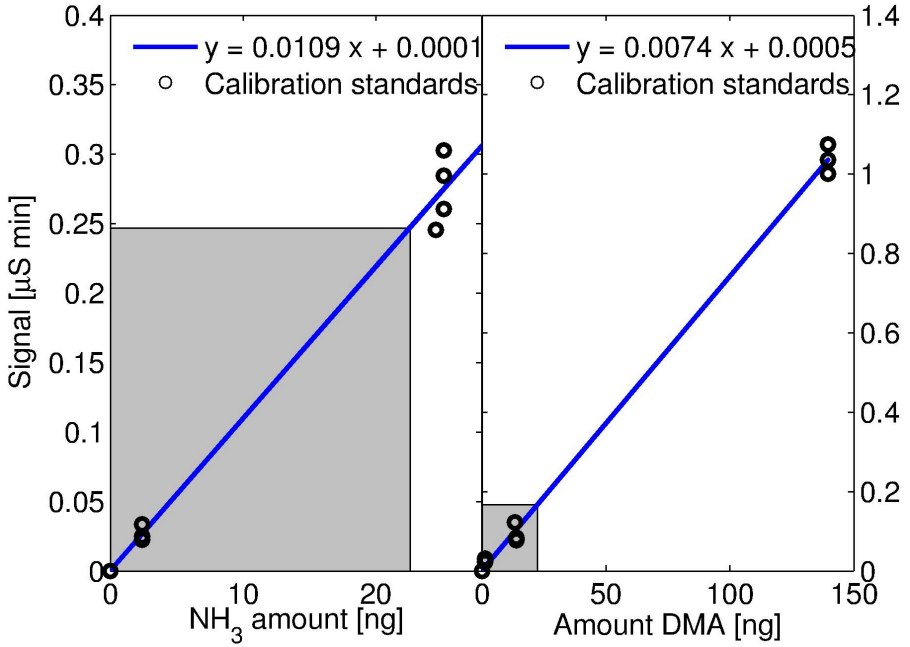

Fig. 3. Calibration plots for ammonia (NH_3, left panel) and dimethylamine (DMA, right panel). Gray areas correspond to the range of experimental data.

AMTD
5, 2395–2413, 2012

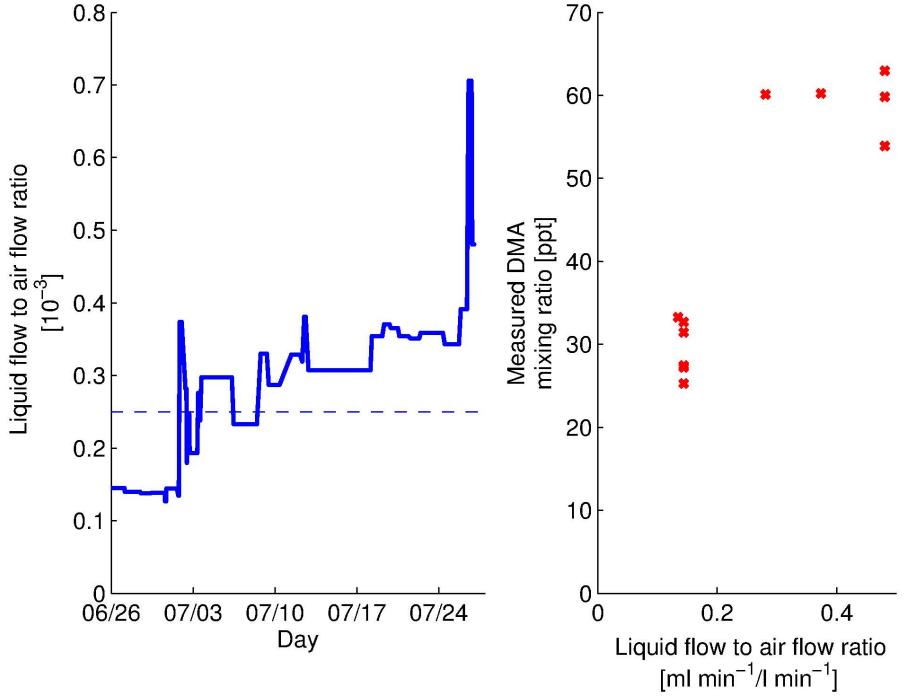

Fig. 4. Liquid to air flow ratio from the sampling line used during the campaign (left panel). The dotted line at 0.25 indicates the ratio for which complete sampling of dimethylamine (DMA) occurs. Measured mixing ratio varying the liquid to air flow ratio while sampling a constant DMA concentration (around 60 pptv) in the chamber (right panel).

AMTD
5, 2395–2413, 2012

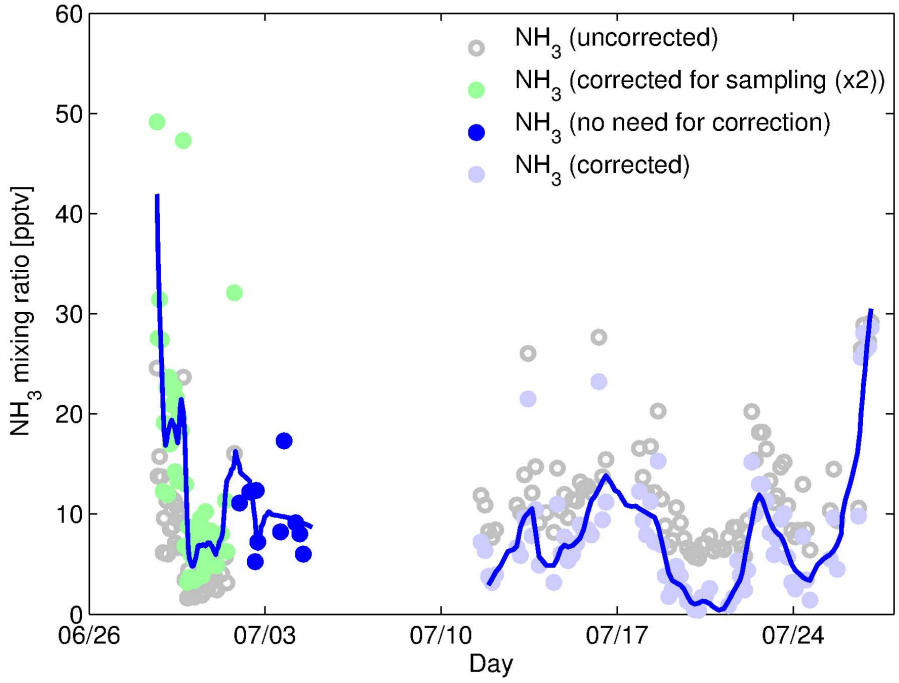

Fig. 5. Overview of ammonia (NH_3) mixing ratios (in pptv): uncorrected (gray), corrected for sampling efficiency (before 1 July, green), without correction required (1 to 6 July, dark blue) and corrected for background levels (after 11 July, light blue). The continuous line is a smoothing function through the final data.

AMTD
5, 2395–2413, 2012

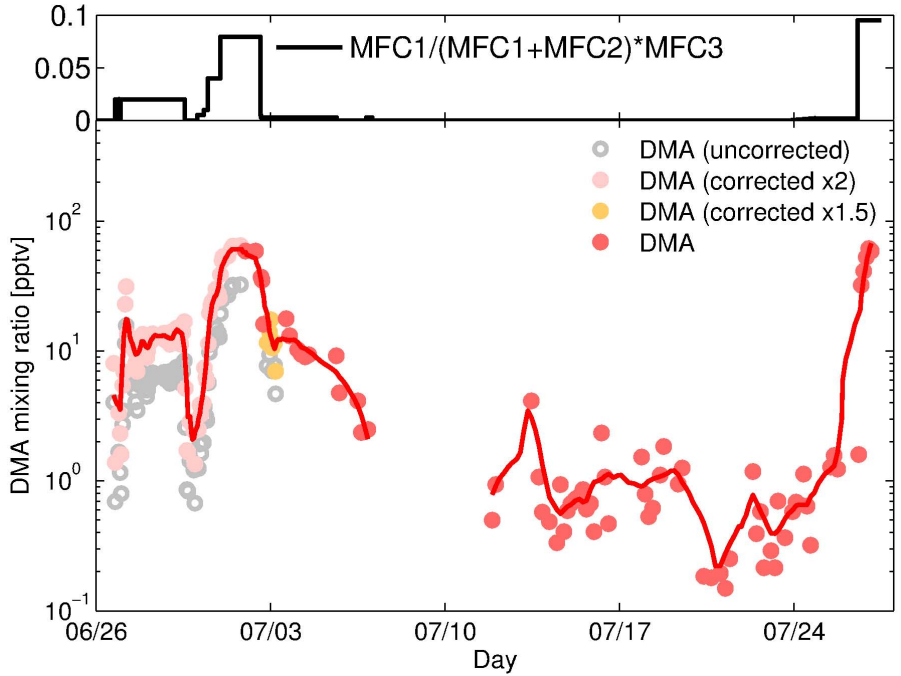

Fig. 6. Mass flow controllers (MFC) settings (top panel) and summary of dimethylamine (DMA) mixing ratio (in pptv) measured (lower panel). A logarithmic scale was used to visualise the data of the second half of the campaign (around 1 pptv).

AMTD
5, 2395–2413, 2012